One Dimensional Charge Fluctuation-Mediated Attraction In High-Tc Superconductor $YBa_2Cu_3O_{7-x}$

Seiichi SEKI

One Dimensional Charge Fluctuation-Mediated Attraction In High-Tc Superconductor $YBa_2Cu_3O_{7-x}$

Seiichi SEKI

Abstract

We investigate the contribution of the $O(4)$ levels toward the charge fluctuation-mediated attraction V between charge carriers, the fluctuation occuring in the $Cu(1)-O(1)-O(4)$ linear chains. The magnitude of V is sensitive to the hole concentration n_c in the chains, and the presence of the $O(4)$ levels induces comparatively large values of V in a certain range of n_c.

§1 Introduction

To account for the scaled up values of the superconducting critical temperature in Cu-O based compounds, many authors have proposed various mechanisms including, for example, the excition,[1]-[4] plasmon,[5]-[6] and antiferromagnetic spin fluctuation[7] mediated pairing models, along with the conventional phonon-model. However, in spite of such accumulated investigations it appears that much work has still to be done before a detailed understanding of the phenomenon.

At its low temperature phase, the crystal structure of high-T_c compound $YBa_2Cu_3O_{7-x}$ indicates the simultaneous presence of the 1D $Cu(1)-O(1)$ chains and 2D $Cu(2)-O(2,3)$ planes, $Cu(1)$ and $Cu(2)$ being bridged with $O(4)$ atoms.[8]-[9] Although the current is mainly carried by holes on the 2D Cu-O planes, the phenomenon of high-T_c superconductivity is observed only in

the presence of the 1D Cu-O chains. This fact may be of primary importance in understanding the large T_c and motivates us to study the relation of such a structure with the occurrence of superconductivity. The purpose of this paper is to investigate the contribution of the O(4) levels toward enhancing the effective attraction between charge carriers, the attraction being caused by the charge fluctuations in the 1D Cu-O chains. Although the charge fluctuation-mediated pairing mechanisms have already been discussed in a number of papers in the context of the excition, plasmon, or charge transfer mediated pairing model,[4] the contribution of the O(4) levels has not yet been studied in detail in the same context. For example, Varma et al[4] have discussed the attraction due to scattering of electrons from excitonic resonances which occur on the current sheets (i.e. on the 2D Cu(2)-O(2,3) planes) and be indifferent to the O(4) levels. In this paper we aim at studying how the presence of the O(4) levels coupled to the levels in the 1D Du(1)-O(1) chains modifies the effective attraction, depending on the position of the Fermi enery in the chains.

The O(4) ions play the role of the junction between Cu(1) and Cu(2). However the Cu(1)-O(4) distance (1.8A) is much shorter than the Cu(2)-O(4) distance (2.3A), and this structural feature makes the bonding of Cu(1) and O(4) stronger than that of Cu(2) and O(4). Thus in discussion of the density of states (DOS) it would be a reasonable starting point to regard that the 1D Cu-O chains are composed of Cu(1), O(1) and O(4) ions.[10] In a tight binding picture, the DOS of such a Cu(1)-O(1)-O(4) linear chain is described by the three subbands, i.e. the bonding and antibonding subbands and the narrow oxygen-dominant (OD) subband. The bonding and antibonding bands are mainly constructed from the Cu(1) and O(1) levels, and both of them show the large 1D dispersion. On the other hand, the OD band results from the coupling of the O(4) and O(1) levels via the Cu(1) sites and/or

from the direct hopping $\tilde{t}$ between the nearest neighbor O(4) and O(1) sites. If the direct hopping is neglected, the OD bandwidth W_0 is approximately equal to the difference between the site-potential energies at O(1) and O(4), $\Delta E = |E_{0(1)} - E_{0(4)}|$, while for the vanishing ΔE, W_0 is of the order of $\tilde{t}$. It is reported that the electron occupation number of the p-state at O(1) is slightly smaller than that at O(4).[1] The difference is about 0.03 per ion, and this suggests the non-vanishing ΔE(0.2eV). $\tilde{t}$ is also considered to be of the same order as ΔE.

For the present material, the bonding and antibonding bands are entirely occupied and unoccupied by electrons, respectively. The OD band is also fully occupied by electrons, but, it appears that the occupation is not complete. Thus the Fermi energy may be near the top of the OD band whose lower and upper edges display the square-root singularity (refer the later discussion), suggesting the large DOS (of the 1D Cu-O chains) at the Fermi energy. This appears to be consistent with the electronic structure calculated by Mattheiss et al[2]. Indeed their calculation indicates that the oxygen levels in the 1D Cu-O chains yield a sharp peak in the DOS near the Fermi enery. In such a situation, the intraband and interband transitions are very sensitive to the position of the Fermi enery E_F in the chains. This implies the conspicuous E_F-dependence of the attraction. We also aim at invesigating such a dependence, in addition to a study of the O(4) levels.

§2　Hole states in the single Cu(2)-O(2 3) plane

Before discussing the charge fluctuations in the Cu(1)-O(1)-O(4) linear chains, we briefly consider the hole states in the single Cu(2)-O(2,3) plane model. In the framework of a tight-binding picture the Hamiltonian can be expressed as

$$H = H_0 + H_{\text{Coulomb}},　　　　　　　(2.1)$$

with the one-particle and Coulomb repulsion terms H_0 and H_{Coulomb} given by

$$H_0 = E_{cu} \sum_{ts} d_{ts}^+ d_{ts} + E_{0,a} \sum_{ms} a_{ms}^+ a_{ms} + E_{0,} \sum_{ns} b_{ns}^+ b_{ns}$$
$$+ t_a/2 \sum_{<tm>s} (d_{tr}^+ a_{ms} + h.c.) + t_b/2 \sum_{<tn>s} (d_{ts}^+ b_{ns} + h.c.)$$
$$+ t_{ab}/4 \sum_{<mn>s} (a_{ms}^+ b_{ns} + h.c.) , \qquad (2.2)$$

and

$$H_{\text{Coulomb}} = U_{ct}/2 \sum_{ts} n_{ts}^d n_{t-s}^d + U_{0x}/2 \sum_{ms} n_{ms}^a n_{m-s}^a$$
$$+ U_{0x}/2 \sum_{ns} n_{ns}^c n_{n-s}^b + V_c \sum_{<tm>} \sum_{s ts z} n_{ts1}^d n_{msz}^a$$
$$+ V_c \sum_{<tn>} \sum_{s ts z} n_{ts1}^d n_{nsz}^b . \qquad (2.3)$$

Here the operators d_{ts}^+, a_{ms}^+ and b_{as}^+ create s-spin holes at Cu(2), O(2) and O(3) sites, respectively, and the symbol $<\ >$ stands for a pair of nearest-neighbor sites. U_{cu} and U_{ox} represent the magnitudes of the Coulomb repulsions at Cu(2) and O(2,3) sites, and V_c is the intersite Coulomb repulsion between the neighboring Cu and O holes with n_{ts}^d, n_{ms}^a and n_{ns}^b being the hole number operators at Cu(2), O(2) and O(3) sites, respectively. When $t_a \neq t_b$ and $E \neq E_{0,b}$, the system is in the inplane anisotropic state which is realized in the superconducting phase of the material we are considering. Fourier-transform of H_0 leads to

$$H_0 = E_{cu} \sum_{ks} d_{ks}^+ d_{ks} + E_{0,a} \sum_{ks} a_{ks}^+ a_{ks} + E_{0,b} \sum_{ks} b_{ks}^+ b_{ks}$$
$$+ t_a \sum_{ks} \cos k_a (d_{ks}^+ a_{ks} + h.c.) + t_b \sum_{ks} \cos k_b (d_{ks}^+ b_{bs} + h.c.)$$
$$t_{ab} \sum_{ks} \cos k_a \cos k_b (a_{ks} + h.c.) , \qquad (2.4)$$

where we have written $k_x d_x$ and $k_y d_y$ simply as k_x and k_y, with the Cu(2)-O(2) and Cu(2)-O(3) distances d_x and d_y. The x and y components of a 2D momentum k are confined to the first Brillouin zone, $-\pi/2 \leq k_x, k_y \leq \pi/2$. The unperturbed Hamiltonian H_0 can be diagonalized by the linear transformation

$$\begin{vmatrix} Q_{1s}^+(k) \\ Q_{2s}^+(k) \\ Q_{3s}^+(k) \end{vmatrix} = U \begin{vmatrix} d_{ks}^+ \\ a_{ks}^+ \\ b_{ks}^+ \end{vmatrix} , \qquad (2.5)$$

and the diagonalized H_0 is given as

$$H_0 = \sum_{j=1, 2, 3} E_j(k) Q_{js}^+(k) Q_{js}(k) , \quad (E_1 < E_2 < E_3) \qquad (2.6)$$

with keeping usual anticommutation rules

$$[Q_{is}(k) , \quad Q_{js}^+(k')]_+ = \delta_{ij}\delta_{kk} , \qquad (2.7a)$$

$$[Q_{is}(k) , \quad Q_{js}(k'))_+ = 0 . \qquad (2.7b)$$

Thus we have the three subbands separated from each other by the finite energy gaps. In the following discussion, the subband specified by the energy E_j in Eq. (2.6) is called the E_j band. Then the E_1 and E_3 bands correspond to the bonding and anti-bonding bands constructed from both the Cu(2) and O(2,3) levels, while the E_2 band is mainly due to the O(2,3) levels and its bandwidth is of the order of t_{ab}. It is a straightforward exercise to derive the equation which determines the eigenenergies $E_j(k)$ for H_0

$$\begin{aligned} Z(E, k) &= (E - E_{cu})(E - E_{0, a})(E - E_{0, b}) - f_k^2(E - E_{0, b}) \\ &\quad - g_k^2(E - E_{0, a}) - [h_k^2(E - E_{cu}) + 2f_k g_k h_k] \\ &= (E - E_1(k))(E - E_2(k))(E - E_3(k)) = 0 , \qquad (2.8) \end{aligned}$$

with $f_k = t_a \cos k_x$, $g_k = t_b \cos k_y$, $h_k = _{ab} \cos k_x \cos k_y$ and $E = E_i(k)$.

At the present stage we apply mean field theoretic treatment to the Coulomb repulsion terms given by (2.3). This is conveniently performed by making use of the transformation (2.5)

$$\begin{vmatrix} d_{ks}^+ \\ a_{ks}^+ \\ b_{ks}^+ \end{vmatrix} = W \begin{vmatrix} Q_{1s}^+(k) \\ Q_{2s}^+(k) \\ Q_{3s}^+(k) \end{vmatrix} , \quad (W = U^{-1}) \qquad (2.9)$$

from which we find the following expressions for the self-energies due to the Coulomb repulsions

$$\begin{aligned} U_{cu}/2 \sum_{is} n_{is}^d n_{i-s}^d &= \tilde{U}_1/2 \sum_{k(>k_F)} \sum_{j=1, 2, 3} \\ &\quad \times |w_{ij}(k)|^2 Q_{js}^+(k) Q_{js}(k) , \end{aligned} \qquad (2.10a)$$

$$U_{0x}/2 \sum_{ms} n_{ms}{}^a n_{m-s}{}^a = \tilde{U}_2/2 \sum_{k(>k_F)} \sum_{j=1, 2, 3}$$
$$\times |w_{2j}(k)|^2 Q_{js}{}^+(k) Q_{js}(k) , \qquad (2.10b)$$

$$U_{0x}/2 \sum_{ns} n_{ns}{}^b n_{n-s}{}^b = \tilde{U}_3/2 \sum_{k(>k_F)} \sum_{j=1, 2, 3}$$
$$\times |w_{3j}(k)|^2 Q_{js}{}^+(k) Q_{js}(k) , \qquad (2.10c)$$

and

$$U_j = \tilde{U}_i \sum_{k(<k_F)} |w_{ji}(k)|^2, \quad (i=1, 2, 3) \qquad (2.11)$$

where w_{ij} are the $i-j$ elements of the matrix W and $U_1 = U_{cu}$ and $U_2 = U_3 = U_{0x}$. The symbol $(k < k_F)$ denotes taking the k-sum inside (outside) the Fermi surface, k_F being the Fermi momentum. We assume that the E_1 band is half-filled at stoichiometry. Then, for the in-plane isotropic case the summation $\sum_{k<k_F)}$ in Eq. (2.11) must be performed within the range

$$|k_x| + |k_y| \leqq \pi/2 , \qquad (2.12)$$

where the equality of the both sides gives the Fermi surface for the half-filled E_1 band. The presence of the small in-plane anisotropy leads to a slight modification of the Fermi surface. Similar procedure is applicable to the V_c-terms in Eq. (2.3), and thus we obtain the following expression for the unoccupied energy levels

$$\tilde{E}_j(k) = E_j(k) + \Delta E_{c, j}(k) , \quad (j=1, 2, 3) \qquad (2.13)$$

with

$$\Delta E_{c, j}(k) = \sum_{i=1, 2, 3} \tilde{U}_i |w_{ij}(k)|^2 + \cdots\cdots , \qquad (2.14)$$

the dots standing for the contribution from the V_c-term. We notice that the $\Delta E_{c, j}$ term gives rise to the so called the Hubbard gap. From numerical evaluation, we have confirmed that $\Delta E_{c, 1}$ becomes much larger than $\Delta E_{c, 2}$ for a set of adequate parameter values ($U_{cu} \sim 8$eV, $U_{0x} \sim 3$eV, $V_c \sim 0.5$eV). This result is easily understood from the fact that the holes in the E_1 band are under the influence of the strong Coulomb repulsions at Cu(2) sites.

Thus the relation, $E_2(k) > E_1(k)$, is satisfied in the wide range of the first Brillouin zone, and then the E_2 band lies inside the Hubbard gap, i.e. the gap between the occupied and unoccupied levels of the E_1 band. In such a situation, the carriers of the supercurrent are mainly in the E_2 band. The Cu(2) and O(3) levels contribute to the DOS of the E_2 band as follows

$$D_{cu(2),\,2}(E) = \sum_k |w_{12}(k)|^2 (E - \widetilde{E}_2(k)) , \qquad (2.15a)$$

$$D_{0(2),\,2}(E) = \sum_k |w_{22}(k)|^2 \delta(E - \widetilde{E}_2(k)) , \qquad (2.15b)$$

$$D_{0(3),\,2}(E) = \sum_k |w_{32}(k)|^2 \delta(E - \widetilde{E}_2(k)) . \qquad (2.15c)$$

whicn are depicted in Fig. 1. In this figure, the solid and dashed curves give $D_{0(2),\,2} + D_{0(3),\,2}$ and $C_{cu(2),\,2}$, respectively, and the curves (a) and (b) correspond to the in-plane isotropic and anisotropic states. For the in-plane isotropic case, $D_{0(2),\,2}$ and $D_{0(3),\,2}$ give the square-root divergence at the upper edge of the E_2 band, while for the in-plane anisotropic case another square-root divergence appears near the upper edge, along with the divergence at the band edge.[3] On the contrary, $D_{cu(2)}$ takes small values in the whole range of the E_2 band, suggesting the small contribution of the Cu(2) holes to the supercurrent.

§3 1D charge fluctuations in the Cu(1)-O(1)-O(4) chains

In this section, we consider the single 2D Cu-O plane and its neighboring layer composed of the 1D Cu-O chains. A hole picture is employed, and holes on the 2D Cu(2)-O(2,3) plane and on the 1D Cu(1)-O(1)-O(4) chains are called 2D and 1D holes, respectively.

The Coulomb interactions between the 2D and 1D holes can be expressed as

$$H_{int} = \sum_{ij} \sum_{ss} U_{ij} n_{is} \bar{n}_{js} , \qquad (3.1)$$

where n_{is} and $\bar{n}_{js}$ are the number operators of 2D and 1D holes, respectively, with site and spin indices, i, j and s, s', and the
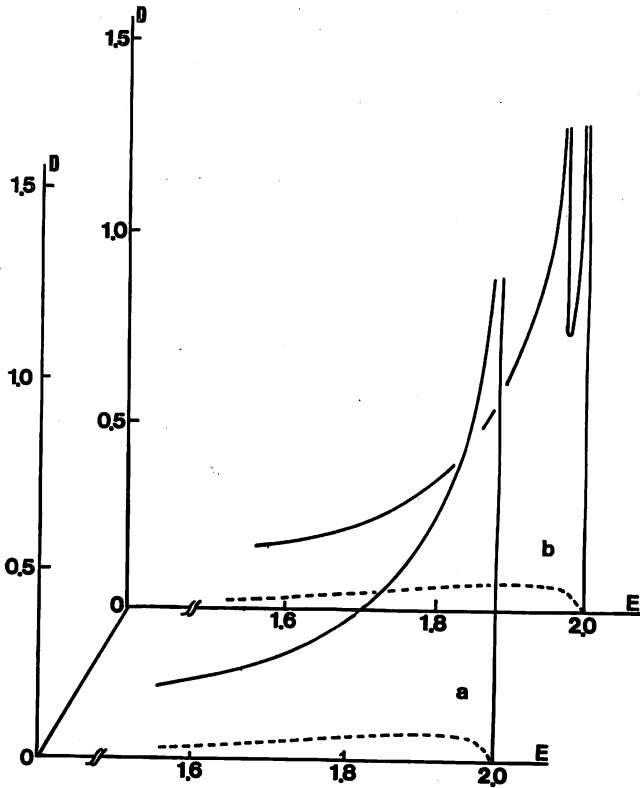
Fig. 1. DOSs defined by Eqs. (2.15a, b). The solid and dashed curves correspond to $D_{O(2),2}+D_{O(3),2}$ and $D_{Cu(2)}$ respectively. $E_{Cu}=0$, $t_{ab}=1$ and $t_a=t_b=1.5$ in unit of eV, and $E_{O(2)}=E_{O(3)}=2$, for (a) and $E_{O(2)}=E_{O(3)}+0.1=2$ for (b).

magnitudes of the Coulomb interactions, U_{ij}. As seen in the preceeding section, the dominant charge carriers are the holes in the E_2 band mainly composed of the O(2,3) levels. This implies the necessity of considering the Coulomb interactions of the O(2,3) holes with the holes in the 1D Cu(1)–O(1)–O(4) chains. In the following discussion, we consider the interactions only with the neighboring Cu(1), O(1) and O(4) holes, although the shielded Coulomb repulsions are still of long range nature. The
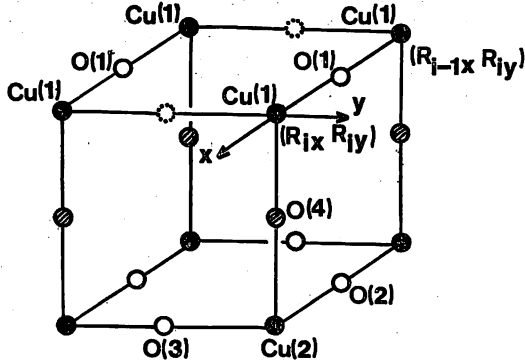
Fig. 2. 2D $Cu(2)-O(2,3)$ and 1D $Cu(1)-O(1)$. $Cu(1)$ and $Cu(2)$ are bridged with $O(4)$.

situation is illustrated in Fig. 2 where the Cu–O layers are spanned by the x and y axes, with the $Cu(1)$-$O(1)$-$O(4)$ chains directed to the x axis. In an oversimplified treatment, the shielded Coulomb interactions are estimated in terms of the factor, $e^2 \exp(-k_s r)r^{-1}$, the notations used being standard. In the framework of the Thomas-Fermi approximation, the shielding parameter k_s is given by $k_s^2 = 4(3/\pi)^{1/3}n_c^{1/3}/a_0$ with the concentration of the charge carriers n_c and the Bohr radius a_0. For the present material, $n_c \sim 5 \times 10^{21}$ cm^{-2} and the $Cu(2)$-$Cu(1)$ and $Cu(2)$-$O(2,3)$ distances are roughly $4A$ and $2A$, respectively. Thus, in a rough estimate the magnitudes of the hole-hole repulsions are given by $U_{O(2)-O(4)} = U_{O(3)-O(4)} \sim 0.4$ eV, $U_{O(2)-Cu(1)} = U_{O(3)-Cu(1)} \sim 0.2$ eV and $U_{O(2)-O(1)} \sim 0.25$ eV. Since the $O(3)$-$O(1)$ distance is much longer than the $O(2)$-$O(1)$ distance, we neglect $U_{O(3)-O(1)}$.

We are now in a position of introducing the explicit expressions for the Coulomb interactions between the 2D and 1D holes. In terms of the $Cu(1)$, $O(4)$ hole creation operators $\bar{d}_{ps}^+$, $\bar{a}_{ps}^+$ and $\bar{b}_{ps}^+$ with 1D mometum p directed to the x-axis and spin s, Fourier-transform of the Coulomb repulsions between the neighboring $O(2,3)$ and $O(4)$ holes can be expressed as

$$H_{int,\,1} = 2U_{O(2)-O(4)} \sum_{R_{iy}} \sum_{k_1,k_2} \sum_{ss'} \cos q \, \delta(k_{2x}-k_{1x}-q)$$
$$\times \exp[-i(k_{1y}-k_{2y})R_{iy}] a_{k_1s}^+ a_{k_2s} \bar{c}_{ps}^+(R_{iy}) \bar{c}_{p-qs}(R_{iy})$$
$$+ 2U_{O(3)-O(4)} \sum_{R_{iy}} \sum_{k_1,k_2} \sum_{ss'} \delta(k_{2x}-k_{1x}-q)$$
$$\times \exp[-i(k_{1y}-k_{2y})R_{iy}] b_{k_1s}^+ b_{k_2s} \bar{c}_{ps}^+(R_{iy}) \bar{c}_{p-qs}(R_{iy}) \qquad (3.2)$$

with 2D momenta $k_1 = (k_{1x}, k_{1y})$ and $k_2 = (k_{2x}, k_{2y})$, and 1D mometa p and q directed to the x axis. Here we have written pL_x and qL_x simply as p and q, L_x being the Cu(1)-O(1) distance. The variable R_{iy} specifies the positions of the 1D Cu-O chains, and thus $\bar{c}_{ps+}(R_{iy})$ creates a O(4) hole at the R_{iy}-chain. Since in the present model, the 1D charge fluctuations can travel only along the x direction, the y-component of the momentum of a 2D hole is unchanged in the 1D charge fluctuation emission and absorption processes. Dirac's delta function in (3.2) indicates momentum conservation in the x direction, with q representing the momentum carried by the 1D charge fluctuations. Similarly, we have the following Coulomb interactions,

$$H_{int,\,2} = 2U_{O(2)-Cu(1)} \sum_{R_{iy}} \sum_{k_1,k_2} \sum_{ss'} \cos q \, \delta(k_{2x}-k_{1x}-q)$$
$$\times \exp[-i(k_{1y}-k_{2y})R_{iy}] a_{k_1s}^+ a_{y_2s} \bar{d}_{ps}^+(R_{iy}) \bar{d}_{p-qs}(R_{iy}), \qquad (3.3)$$

$$H_{int,\,3} = 2U_{O(3)-Cu(1)} \sum_{R_{iy}} \sum_{k_1,k_2} \sum_{ss'} \delta(k_{2x}-k_{1x}-q)$$
$$\times \exp[-i(k_{1y}-k_{2y})R_{iy}] b_{k_1s}^+ b_{k_2s} \bar{d}_{ps}^+(R_{iy}) \bar{d}_{p-qs}(R_{iy}), \qquad (3.4)$$

$$H_{int,\,4} = 2U_{O(2)-O(1)} \sum_{R_{iy}} \sum_{k_1,k_2} \sum_{ss'} \delta(k_{2x}-k_{1x}-q)$$
$$\times \exp[-i(k_{1y}-k_{2y})R_{iy}] a_{k_1s}^+ a_{k_2s} \bar{a}_{ps}^+(R_{iy}) \bar{a}_{p-qs}(R_{iy}). \qquad (3.5)$$

The above Hamiltonians yield the various 1D charge fluctuation emission and absorption processes of the holes in the E_2 band. Each process is described by the relevant three point vertices as depicted in Figs. 3 (a) and (b) where the solid and wavy lines represent the propagators of the E_2 holes and the 1D charge fluctuations, respectively. In the lowest order, the Coulomb repulsions (3.2-5) give rise to the vertices,

$$\Gamma_{O(2)-Cu(1)}(k, k-q\,;\,q) = 2U_{O(2)-Cu(1)} g_{22}(k, k-q) \cos q, \qquad (3.6\,\text{a})$$

$$\Gamma_{O(2)-O(1)}(k, k-q\,;\,q) = U_{O(2)-O(1)} g_{22}(k, k-q), \qquad (3.6\,\text{b})$$

$$\Gamma_{O(2)-O(4)}(k, k-q\,;\,q) = 2U_{O(2)-O(4)} g_{22}(k, k-q) \cos q, \qquad (3.6\,\text{c})$$
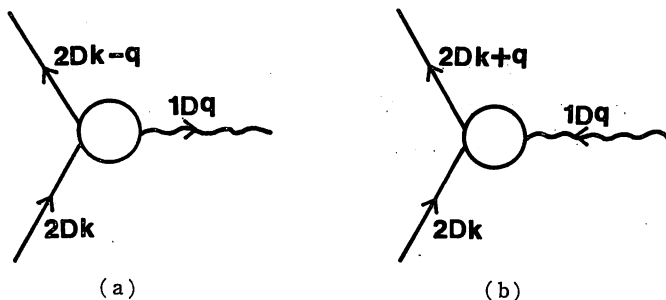
Fig. 3. Three point vertices for the 1D charge fluctuation emission (a) and absorption (b) processes due to the E_2 holes.

and

$$\Gamma_{0(3)-Cu(1)}(k, k-q; q) = 2U_{0(3)-Cu(1)}g_{32}(k, k-q), \qquad (3.7a)$$

$$\Gamma_{0(3)-0(1)}(k, k-q; q) = 2U_{0(3)-0(1)} = 0, \qquad (3.7b)$$

$$\Gamma_{0(3)-0(4)}(k, k-q; q) = 2U_{0(3)-0(4)}g_{32}(k, k-q), \qquad (3.7c)$$

where $g_{ij} = w_{ij}(k)w_{ij}(k-q)$ with the $i-j$ components w_{ij} of the matrix W defined by Eq. (2.9). As is easily understood from Eq. (2.9), the factors g_{22} and g_{32} in Eqs. (3.6) and (3.7) come from taking the Q_2 component of the original fermion operators a^+ and b^+. We neglect the Coulomb interactions of the Cu(2) holes with the neighboring O(4), Cu(1) and O(1) holes, since the contribution of the Cu(2) levels to the E_2 band is extremely small as illustrated in Fig. 1. Making use of (3-6) and (3.7), the effective couplings of the E_2 holes with the Cu(1), O(1) and O(4) holes can be described by the following three point vertices, respectively,

$$\gamma_1 = \Gamma_{0(2)-Cu(1)} + \Gamma_{0(3)-Cu(1)} \qquad (3.8a)$$

$$\gamma_2 = \Gamma_{0(2)-0(1)} + \Gamma_{0(3)-0(1)}, \qquad (3.8b)$$

$$\gamma_3 = \Gamma_{0(2)-0(4)} + \Gamma_{0(3)-0(4)}. \qquad (3.8c)$$

To investigate the scattering processes of the 2D holes from the 1D charge fluctuations, we need to clarify the properties of the 1D charge fluctuations. For this purpose, we introduce the

unperturbed Hamiltonian for a single 1D Cu(1)-O(1)−O(4) chain,

$$H_{0,1D} = E_d \sum_{ts} \bar{d}_{ts}{}^+ \bar{d}_{ts} + E_{0(1)} \sum_{js} \bar{a}_{js}{}^+ \bar{a}_{js} + E_{0(4)} \sum_{ts} \bar{c}_{ts}{}^+ \bar{c}_{ts}$$
$$+ \sum_{<tj>s} t_{tj} (\bar{d}_{ts}{}^+ + h.c.) + \sum_{ts} \bar{t} (\bar{d}_{ts}{}^+ \bar{c}_{ts} + h.c.)$$
$$+ \sum_{ts} \tilde{\bar{t}} (\bar{a}_{ts}{}^+ \bar{c}_{ts} + h.c.). \qquad (3.9)$$

Here we have neglected the index R_{ty} of the fermion operators. Fourier-transforming the 1D Hamiltonian (3.9), we easily find that the three eigenenergies $\bar{E}_1$, $\bar{E}_2$ and $\bar{E}_3$ $(\bar{E}_1 > \bar{E}_2 > \bar{E}_3)$ of $H_{0,1D}$ satisfy

$$E - E_d = [f_k{}^2 + \{g_k{}^2 (E_{0(1)} - E_d) + 2\bar{t} f_k g_k\} (E_{0(1)} - E_{0(4)})^{-1}] (E - E_{0(1)})^{-1}$$
$$+ [t^2 + \{g_k{}^2 (E_{0(4)} - E_d) + 2\bar{t} f_k g_k\} (E_{0(4)} - E_{0(1)})^{-1}] (E - E_{0(4)})^{-1}, \quad (3.10)$$

with $f_k = 2t \cos k_x$ and $g_k = 2\tilde{t} \cos k_x$. Here, $\bar{E}_1$ and $\bar{E}_2$ are the energies for the bonding (B) and antibonding (AB) subbands and $\bar{E}_2$ is the energy for the oxygen-dominant (OD) subband. Then we can easily prove that the DOS_s for these subbands are given by the following common expression (with different energy ranges)

$$D(E) = \pi^{-1} \{I(E)(1-I(E))\}^{-1/2} |F(E)|^{-1} |3E^2 - 2(E_d + E_{0(1)}$$
$$+ E_{0(4)})E + E_d E_{0(1)} + E_{0(1)} E_{0(4)} + E_{0(4)} E_d - \bar{t}^2 - 4(\tilde{t}^2 + t^2) I(E)|$$
$$\times \theta(I(E))\theta(1-I(E)), \qquad (3.11)$$

where

$$I(E) = \{(E - E_d)(E - E_{0(1)})(E - E_{0(4)}) - \bar{t}^2 (E - E_{0(1)})\} \{F(E)\}^{-1}, \qquad (3.12)$$

and

$$F(E) = 4\{t^2 (E - E_{0(4)}) + \tilde{t}^2 (E - E_d) + 2\tilde{t} t \bar{t}\}, \qquad (3.13)$$

with Heaviside's unit step function θ. Combination of Eqs. (3.12) and (3.13) allows us to state that each subband has the square-root divergence at its lower and upper band edges. The DOS for the 1D Cu-O chain is depicted in Fig. 4 where the solid-dot, dashed and dotted curves represent the contribution from the
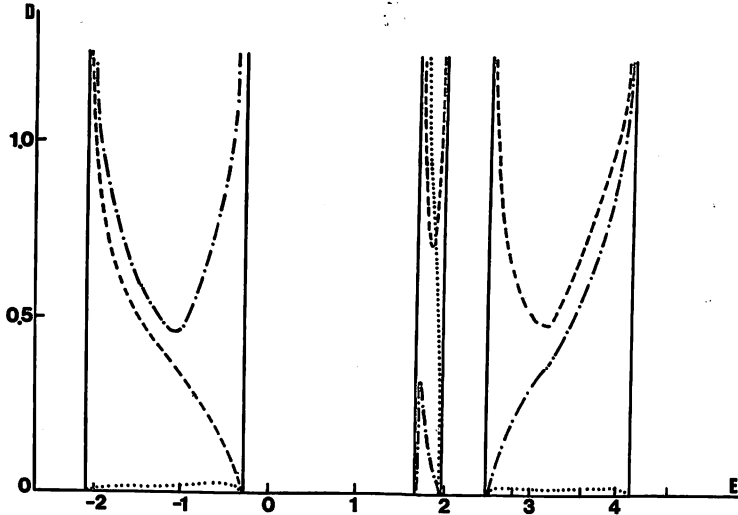
Fig. 4. DOSs for the B, OD and AB bands specified by the energies $\bar{E}_1$, $\bar{E}_2$ and $\bar{E}_3$ (Eqs. (3.11a, b, c)), respectively. The solid-dot, dashed, and dotted curves represent the contributions from the Cu(1), O(1), and O(4) states. $\bar{E}_d=0$, $E_{0(1)}=2$, $E_{0(4)}=2.2$, $t=1.5$, $\bar{t}=0.8$ $\tilde{t}=0$ in unit of eV. The small but non-zero $\tilde{t}$ leads to the similar curves for the DOS.

Cu(1), O(1) and O(4) levels, respectively. This figure exhibits that the B and AB bands are mainly composed of the Cu(1) and O(1) levels, whereas the OD band is mainly due to the O(4) and O(1) levels. Thus, the interband B→OB and OD→AB and intraband OD→OD transitions would partly accompany the O(1)↔O(4) transitions. It is worth noting that in the absence of the O(4) levels, the DOS is constructed only from the B and AB bands; then the particle-hole excitations are realized only by the B→ AB trausitions.

To calculate the 1D charge fluctuations, we introduce the following single particle Green functions,

$$G_p{}^{mn}(E) = \sum_{Rjx} \int dt \exp[i(pR_{jx}-Et)] < TA_{is}{}^m(t)A_{js}{}^{n+}(0) >,$$

$$(3.14)$$

where $m, n = 1, 2, 3$ and $A_{ts}^1 = \bar{d}_{ts}, A_{ts}^2 = \bar{a}_{ts}$ and $A_{ts}^3 = \bar{c}_{ts}$. Then particle-hole excitations can be described by product of two Green functions

$$\chi_0^{mn}(q, q_0) \sum_p dE \, G_{p+q/2}^{mn}(E+q_0/2) G_{p-q/2}^{mn}(E-q_0/2), \quad (3.15)$$

carrying momentum q and energy q_0. It is convenient for our purpose to write $G_p^{mn}(E)$ as

$$G_p^{mn}(E) = \sum_{j=1,2,3} Z_j^{mn}(p) \left\{ \frac{\theta(E_j(p) - E_F)}{E - E_j(p) + E_F + i\delta} + \frac{\theta(E_F - E_j(p))}{E - E_j(p) + E_F - i\delta}, \right. \quad (3.16)$$

with the Fermi energy E_F. Z_j^{mn} represents the wavefunction renormalization and be given by

$$[Z_j^{mn}(p)]^{-1} = \lim_{E \to E_j(p)} G_p^{mn}(E)/(E - E_j(p)). \quad (3.17)$$

Then substitution of Eq. (3.14) into Eq. (3.15) leads after a few manipulations to the following expression for the real and imaginary parts of $\chi_0^{mn}(q, q_0)$,

$$Re[\chi_0^{mn}(q, q_0)] = P \sum_i \sum_j \int dp \, Z_i^{mn}(p+q/2) Z_j^{mn}(p-q/2)$$
$$\times \frac{\theta(E_i(p) - E_F) - \theta(E_F - E_i(p))}{q_0 - E_i(p+q/2) + E_j(p-q/2)}, \quad (3.18)$$

$$Im[\chi_0^{mn}(q, q_0)] = \sum_i \sum_j \int dp \, Z_i^{mn}(p+q/2) Z_j^{mn}(p+q/2)$$
$$\times \theta(E_i(p) - E_F) \theta(E_F - E_i(p)) \delta(q_0 - E_i(p+q/2)$$
$$+ E_j(p-q/2)). \quad (3.19)$$

The factor P in Eq. (3.18) denotes taking the principle value.

To proceed further analysis, we introduce the Hubbard type interaction (within each 1D Cu-O chain) defined in such a way that

$$H_c = U_{cu}/2 \sum_{ts} \bar{d}_{ts}^+ \bar{d}_{t-s}^+ \bar{d}_{t-s} \bar{d}_{tx} + U_{0x}/2 \sum_{js} \bar{a}_{js}^+ \bar{a}_{j-s}^+ \bar{a}_{j-s} \bar{a}_{js}$$
$$+ U_{0x}/2 \sum_{ts} \bar{c}_{ts}^+ \bar{c}_{t-s}^+ \bar{c}_{t-s} \bar{c}_{ts}. \quad (3.20)$$

Here we neglect the repulsion between the neighbouring Cu(1) and O(1) (or O(4)) holes, because it is much smaller than the on-site Coulomb repulsion U_{cu} and U_{ox}. To write the formulation in a compact form, we introduce the 3×3 matrices,

$$\chi_0 = \begin{vmatrix} \chi_0^{11} & \chi_0^{12} & \chi_0^{13} \\ \chi_0^{21} & \chi_0^{22} & \chi_0^{23} \\ \chi_0^{31} & \chi_0^{32} & \chi_0^{33} \end{vmatrix}, \qquad U = \begin{vmatrix} U_{cu} & 0 & 0 \\ 0 & U_{ox} & 0 \\ 0 & 0 & U_{ox} \end{vmatrix}. \tag{3.21}$$

Then, the chain approximation yields the following expression for the $m-n$ component of the 1D chorge fluctution matrix χ

$$\chi^{mn} = \chi_0^{mn} + \sum_{i,j} \chi_0^{mi} U^{ij} \chi_0^{jn} + \sum_{i,j,k,l} \chi_0^{mi} U^{ij} \chi_0^{jk} U^{kl} \chi_0^{ln}$$
$$+ \dots, \tag{3.22}$$

where the dots stand for the higher order terms with respect to the Coulomb repulsions. From Eq. (3.22) it follows that

$$\chi^{mn} = \{(1-\chi_0 U)^{-1}\chi_0\}_{mn}, \tag{3.23}$$

where $(M)_{ij}$ denotes the (i,j)-component of the 3×3 matrix M.

The densities of states for the 1D charge fluctuations χ^{mn} are given by

$$F_{mn}(q, q_0) = 2Im[\{(1-\chi_0 U)^{-1}\chi_0\}_{mn}], \tag{3.24}$$

where Im means taking the imaginary part. F_{mn} gives distribution of the eigenenergies of the corresponding charge fluctuation. The factor 2 in Eq. (3.24) comes from the summation over the spin index. In Figs. 5(a) and (b), we present the particle-hole continum where F_{ij} is non-vanishing in the $q-q_0$ plane. We notice that in the hole picture we are using, the Fermi energy E_F is considered to be inside the gap between the B and OD bands or near the lower edge of the OD band. Figure 5(a) cerresponds to the case of E_F lying inside the gap between the B and OD bands, and then the particle-hole excitations are realized only by the interband B→OD and B→AB transitions. These excitations take comparatively high frequencies, owing to the large energy gaps.
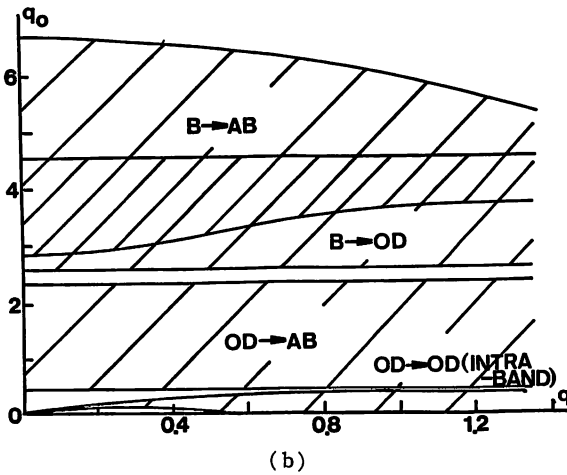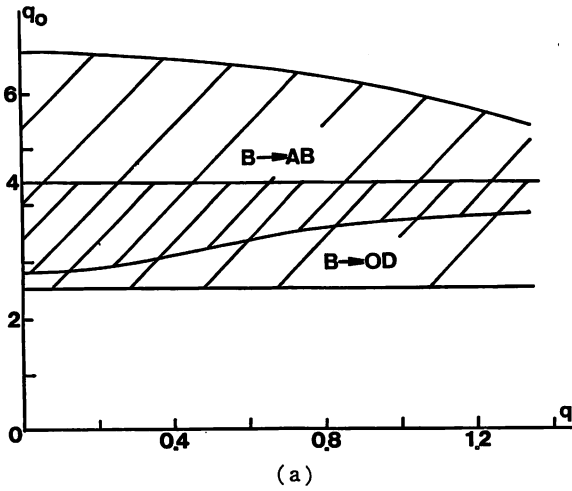
Figs. 5. (a) and (b)
Particle-hole continuum. In the hatched region, the imaginary part of the fluctuation is non-zero. Parameter values are the same as those employed in Fig. 4. (a) E_F lies inside the gap of the B and OD bands. (b) E_F lies inside the OD band; $E_F=2.05eV$.

On the other hand, for E_F lying inside the OD band, the intraband (OD→OD) and interband (OD→AB) transitions take place, along with the B→AB and B→OD transitions (Fig. 5(b)). Since the OD band is close to the AB band, the particle-hole excitations due to the OD→AB transitions take smaller energies or equivalently
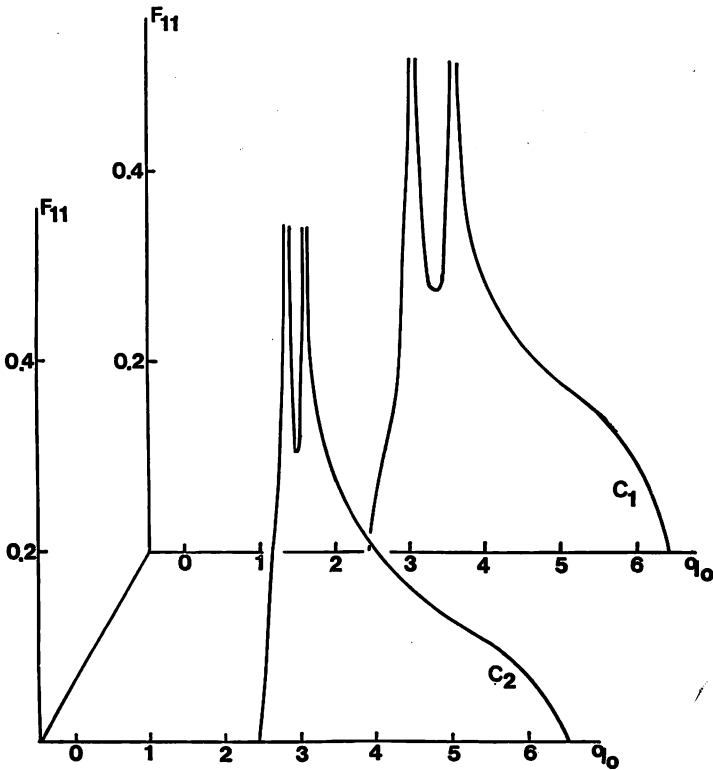
(a)

Figs. 6. (a) and (b)

   Energy q_0 dependence of the spectrum F_{11}. Parameter values are the same as those employed in Fig. 5. (a) E_F lies inside the gap of the B and OD bands. (b (E_F lies inside the OD band; $E_F=2.05$eV. $U_d=8$eV and $U_0=3$eV. The curves C_1 and C_2 correspond to $q=0.1$ and 0.6, respectively.

lower frequencies than those due to the B→AB and B→OD transitions. We depict the 1-1 component of F_{ij}, i.e. F_{11} in Figs. 6(a) and (b) where E_F lies inside the gap between the B and OD bands for (a) and inside the OD and for (b). The sharp peaks in the spectrum correspond the charge transfer excitonic reson-ances. In Fig. 6(a) we find two sharp peaks corresponding to the B→OD and B→AB transitions (in order of lower energy), while in Fig. 6(b) there appear four peak corresponding to the OD→OD, OD→AB, B→AB, and B→AB transitions. The other components of F_{ij} behave like F_{11} in the gross features.
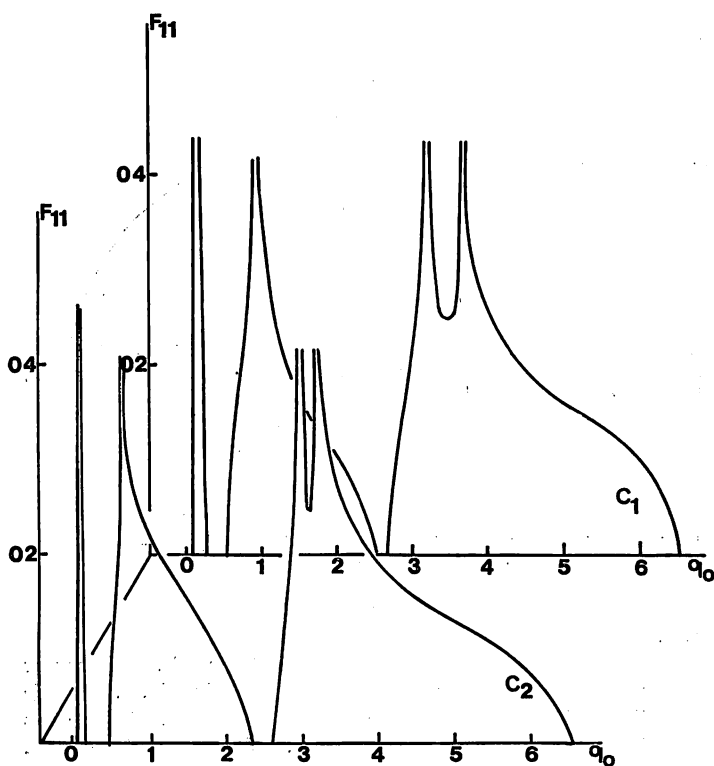
(b)

As for the attractive interaction due to scattering of electrons from excitonic resonances, Allender, Bray and Bardeen[3] have derived the approximate relation, $V \sim \mu/F\omega_p{}^2, \omega_g{}^2$, where μ is the repulsion between electrons and F is the specrtum of the particle-hloe excitations with ω_p and ω_g being the plasmon energy and the energy gap. However this formula is not necessarily convenient for the present model, since in our discussion the various interband and intraband transitions take place. Thus, instead of the formula obtained by Allender et al, we make use of a slightly different expression which is derived as follows.

In the phonon-mediated pairing mechanism, the attraction V between charge carriers is proportional to the interaction of each carrier with the polarizable medium, g. It is also proportional to the inverse of a typical phonon energy E_{ph}, the inverse indicating how easily the medium is polarizable. Thus we have $V \sim g^2/E_{ph}$. Similar expression is valid for the attraction caused by exchange of boson-like modes other than the lattice vibrations. In the present case, the excitonic resonances have a continum of eigenenergies, which is specified by the spectrum function (3. 24). Thus, it follows that

$$V = \sum_{m,n} \int dEdk < \gamma_m(k, k-q ; q) F_{mn}(q, E) \gamma_n(-k, -k+q ; q) >_{AV}/E,$$
$$(3. 25)$$

where $<...>_{AV}$ means taking the average over 1D momentum q, and the three point vertices γ defined by (3. 6) and (3. 7). In Eq. (3. 25), we have assumed the vanishing total momentum of a Cooper pair. The calculated results are illustrated in Fig . 7, representing the E_F dependence of V. In this figure, the solid and dashed curves correspond to the in-plane isotropic and in-plane anisotropic cases. In this paper, we have introduced the in-plane anisotropy only by the inequalities, $t \neq t_b$ anu $E_{0, a} \neq E_{0, b}$ (refer Eq. (2. 2)), which affect on the value of g_{tt} appearing in the vertices (3. 6) and (3. 7). In such a treatment, the in-plane

anisotropy induces only a small modification of the result for the isotropic case. When E_p lies inside the gap between the B and OD bands, the possible particle-hole excitations are due to the B→OD and B→AB transitions. Then we have $V\sim 0.4$-0.5eV, as illustrated by the flat lines in Fig. 7. With increasing E_F, V increases rapidly toward its maximum and then decreases gradually. When the small amount of holes occupy the OD band, there occur the particle-hole excitations attributed to the intraband OD→OD and interband OD→AB transitions, in addition to the B→OD and B→AB transitions. Both the OD→OD and OD→AB transitions take comparatively small energies, and they make a large contribution to enhancing the value of V. Indeed, as is seen from (3.25), the excitonic resonances with lower energies are more
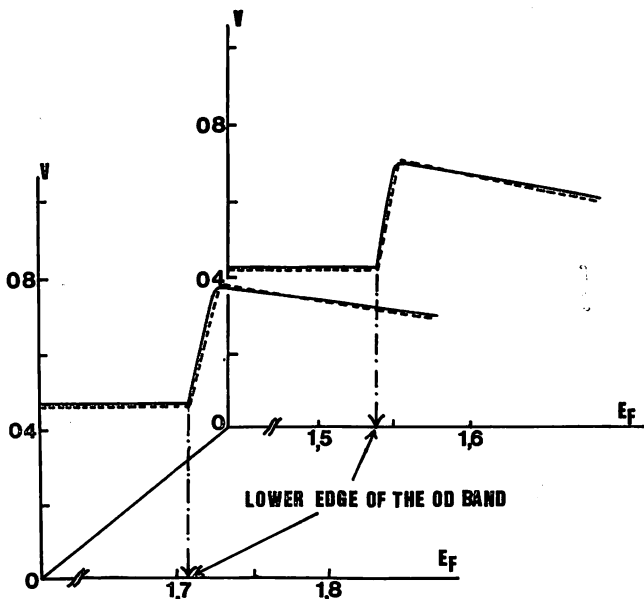
Fig. 7. Fermi energy-dependences of the effective attraction V given by *Eq.* (3.25). The solid and dashed curves correspond to the 2D in-plane isotropic and in-planeanisotropic cases.

favorable than those with higher energies in enhancing V. Thus, the OD→OD and OD←AB transitions are the origin of the rapid increase in the E_F dependence of V. We notice that the maximum of V is about 0.6~0.7eV. Although these values are smaller, for example, than those obtained by Ruvalds[14] using the 2D plasmon-mediated pairing model (V~1-1.4ev), the calculated values still suggests the significant role of the mechanism discussed above.

We notice that the presence of O(4) atoms plays a key role in our discussion. As stated already, in the absence of O(4) the DOS for each 1D Cu-O chain is composed of the bonding and adtibonding bands without the narrow OD band. Then the charge fuctuations stem only from the B→AB transitions, whose contribution toward the attraction is about a half of the values illustrated in Fig. 7.

§4 Summary

In this paper, we have considered the effective attraction induced by the charge fluctuations occurring in the 1D Cu-O chains. Our main concern in this paper has been to discuss contribution of the O(4) levels toward the attraction, and we have stressed the role of the narrow oxygen-dominant band constructed mainly from the coupling of the O(4) and O(1) levels. Freeman et al[10] have also suggested the significance of the O(4) levels coupled to the 1D Cu(1)-O(1) chains, in the framework of the band structural calculation.

In the superconducting phase, the Fermi energy E_F in the hole picture lies i) around the lower edge of the OD band or ii) inside the energy gap between the B and OD bands, and such particular postions of E_F make the charge fluctuations very sensitive to the hole concentration in the Cu-O chains. Our calculation indicates that for both cases i) and ii), the OD band gives a large contribution to enhancing the magnitude of the effective attraction. In particular, for the case i) the electronic transitions OD→OD

and OD→AB take place in the chains, along with those observed for the case ii), and mixing of such transitions makes enhancement of V more conspicuous than the case of i). Furthermore, the $O(2,3)-O(4)$ distance is much shorter than the $O(2,3)-O(1)$ (or $Cu(1)$) distance, and this leads to comparatively large Coulmb interaction between the $O(4)$ and $O(2,3)$ holes, or equivalently, large contribution of the $O(4)$ levels to the three point vertices defined by (3.6) and (3.7).

Use of Morel-Anderson formula[15] leads to $T_c = <E_{flu}> \exp [-(V-\mu)^{-1}]$, where $<E_{flu}>$ is the averaged eigenenergy of the charge fluctuations, and $V(\mu)$ the magnitude of the attractive (repulsive) interaction. This formula indicates that high-T_c superconductivity results from the large $<E_{flu}>$, i-e- high frequencies of particle-hole resonances in addition to the enhanced V. The interband transitions OD→AB and B→AB play a significant role in enhancing the frequencies of the resonances as well as in enhancing V, while the intraband OD→OD and interband B→OD transitions make a comparatively large contribution toward the enhancement of V. Although the introduction of the $O(4)$ levels coupled to the 1D Cu-O chains tends to reduce $<E_{flu}>$, the presence of these levels makes the T_c-value higher via the conspicuous increasing of the effectiue attraction. The detailed discussion will be presented in a separate paper.[16]

References

1) W. A. Little, Phys. Rev. *134* (1964) A1416.

2) V. L. Ginzburg, Phys. Lett., *13* (1964) 201.
   V. L. Ginzburg and D. A. Kirzhnits, Phys. Rep., *4* (1972) 345.

3) D. Allender, J. Bray and J. Bardeen, Phys. Rev., *B7* (1973) 1020.

4) C. M. Varma, S. Schmit-Rink [and Elihu Abrahams, Solid State commun., *62* (1987) 631.

5) E. A. Pashitskii and V. M. Chernovsenko, Sov. Phys. -JETP, *33* (1971) 802.

6) J. Ruvalds, Phys. Rev., *B35* (1987) 8869.

7) V. J. Emery, Phys. Rev. Lett., *58* (1987) 2794.

8) J. J. Capponi, C. Chaillout, A. W. Hewat, P. Lejay, M. Marezio, N. Nguyen, B. Raveau, J. L. Soubeyroux, J. L. Tholence, R. Tourrier, Europhys. Lett., *12* (1987) 1301.

9) M. A. Beno, L. Soderholm, D. W. Capone, D. Hinks, J. D. Jorgensen, I. K. Zhang, J. D. Grace, Appl. Phys. Lett., *51* (1987) 57.

10) A. J. Freeman, Jaejun Yu, S. Massidda, and D. D. Koelling, Physica *148B* (1987) 212.

11) C. Ambrosch-Draxl, P. Blaha, and K. Schwarz, in *Electronic Properties of High–T_c Superconductors and Related Compounds*, Ed. H. Kuzmany, M. Mehring, and J. Fink, Springer-Verlag, 1990, p. 338.

12) L. F. Matteiss and D. R. Hamann, Solid State Commum., *63* (1987) 395.

13) S. Seki, Solid State Commun., *79* (1991) 051.
    S. Seki, Solid State Commun., *79* (1991) 655.

14) J. Ruvalds, Phys. Rev. B, *35* (1987) 8869.

15) P. Morel and P. W. Anderson, Phys. Rev. *125* (1962) 1263.

16) S. Seki, submitted to Prog. Theor. Phys.